Received: 7 February 2023 | Revised: 25 May 2023 | Accepted: 7 July 2023

DOI: 10.1002/rnc.6896

RESEARCH ARTICLE

WILEY

Attitude filtering with uncertain process and measurement noise covariance using SVD-aided adaptive UKF

Chingiz Hajiyev[1] | **Demet Cilden-Guler**[2]

[1]Department of Aeronautical Engineering, Faculty of Aeronautics and Astronautics, Istanbul Technical University, Istanbul, Turkey

[2]Department of Astronautical Engineering, Faculty of Aeronautics and Astronautics, Istanbul Technical University, Istanbul, Turkey

Correspondence
Demet Cilden-Guler, Department of Astronautical Engineering, Faculty of Aeronautics and Astronautics, Istanbul Technical University, 34469 Maslak, Istanbul, Turkey.
Email: cilden@itu.edu.tr

Abstract

It is presented in this article how to simultaneously alter the process and measurement noise covariance matrices for nontraditional attitude filtering technique. The unscented Kalman filter (UKF) and singular value decomposition (SVD) methods are integrated in the nontraditional attitude filtering algorithm to estimate a nanosatellite's attitude with an inherent robustness feature. The SVD approach determines the attitude of the nanosatellite and provides one estimate at a single frame utilizing measurements from the magnetometer and Sun sensor as the initial stage of the algorithm. These attitude terms are subsequently fed into the UKF with their error covariances, which makes the filter robust inherently. The attitude estimations of the satellite are compared between the filters presented. The Q (process noise covariance) adaption approach with multiple scale factors is specifically suggested for differences in between the process channels. Performance of the multiple scale factors-based adaptive SVD-aided UKF is examined in the event of process noise increase, which may result from changes in the environment or satellite dynamics.

KEYWORDS

attitude estimation, magnetometer, multiple measurement scale factor, multiple scale factors, robust unscented Kalman filtering, single-frame estimator, Sun sensor

1 | INTRODUCTION

Sun sensor and magnetometer onboard small spacecraft flying low Earth altitudes are typically used as attitude sensors. Use a Kalman filtering technique to integrate the measurements under the propagation model of the satellite dynamics and estimate the attitude of the satellite as a basic solution for the attitude estimation problem with magnetometer and Sun sensor measurements.

1.1 | Background

The nonlinear measurements of reference directions can be used to create a Kalman filter for satellite attitude and rate estimates in traditional approaches.[1–4] The nonlinear models of the reference directions serve as the foundation for the measurement models in the filter. Therefore, nonlinear equations are used to link the data and states. Magnetometer-only attitude estimation is presented in Reference 1 based on a traditional unscented Kalman filter (UKF) algorithm. The quaternion's unit-constraint is enforced by a dummy measurement of quaternion norms. Another traditional UKF is presented in Reference 2 for estimation of the attitude and external torques. That algorithm is designed based on the magnetometer and rate gyro measurements. Another study in Reference 3 based on the traditional approach that uses sun sensors in addition to the magnetometers and rate gyros presents an attitude estimation of CubeSats. A quaternion estimation using a UKF is presented in Reference 4 based on sun and magnetic field reference directions. SVD method is also used for initial attitude estimate for faster convergence. However, the SVD is neither used for adapting the measurement covariance nor updates the filter at each single-frame. These types of filters are categorized under the traditional approach using nonlinear measurements without having an adaptation in the measurement or in the process noise covariances.

The measurements in the conventional attitude filter may reference the Earth's magnetic field vector or to any of the direction vectors to the Sun, star, etc. To estimate the attitude of the satellite, the simple concept is to compare the vectors measured in the body frame with the known vectors in the inertial (or any other reference) frame.[3,5] When employing the conventional attitude filtering methodology, it is possible to retrieve the initial values for the Kalman filter using a single-frame method.[6] In Reference 7, to conduct a cost–benefit analysis, various spacecraft attitude estimation and determination techniques are studied. The decision between the attitude determination algorithms is examined in terms of the necessary accuracy and computational resources. The classic Kalman filter provides superior estimation accuracy but comes at a larger computational cost than single-frame-based approaches like TRIAD and q-method, which are expectedly characterized by cheap computational cost and deliver poor attitude estimation accuracy. Other methods seek to provide recursive attitude estimates without the use of a filtering technique. In Reference 8, to reduce the Wahba's cost function, an iterative gradient optimization is performed. For a spacecraft with a Sun sensor, magnetometer, and rate gyroscope, the algorithm calculates the quaternions and gyro biases.

The attitude angles are first determined in a nontraditional way based on the linear measurements by employing the vector measurements and an appropriate single-frame attitude determination technique[9–11] at each recursive step. Following that, these attitude angles are utilized directly as measurement inputs for an attitude filter, such as the Extended Kalman filter (EKF) or UKF. Given that the states are being measured directly, the measurement model in this instance is linear. As an example, in Reference 9, the algebraic approach and the EKF algorithms are merged in the authors' integrated satellite attitude determination system to estimate the attitude angles and angular velocities, respectively. The algebraic method is used by the attitude determination system (two-vector algorithm). This approach is based on measuring the same vectors in the body coordinate system after computing any two analytical vectors in the reference frame. Three distinct two-vector algorithms based on the Earth's magnetic field, the Sun vector, and the nadir vector are proposed, and measurement tools include magnetometers, Sun sensors, and horizon scanners/sensors. An EKF, whose measurement inputs are the estimates of the two-vector algorithm, is created in order to acquire the satellite's angular motion parameters with the appropriate accuracy.

The main benefit of the nontraditional strategy for attitude filtering is that it lightens the algorithm's computing burden. The overall processing load for the attitude estimation technique can be greatly reduced because the measurement model for the nontraditional attitude filter is linear. The particular algorithms that make up each stage of the nontraditional attitude filter determine how much of the computational load is reduced in each level. Additionally, compared to estimates from a typical filter, the estimation accuracy may rise if the filter is properly set. These advantages make the nontraditional approach to attitude filtering a potential technique for estimating the attitude of small spacecraft, including nanosatellites.[10,12–15]

1.2 | Related studies

When compared to a filter that adjusts the measurement noise covariance matrix (R matrix) based on the innovation sequence, the nontraditional technique has the capacity to be robust against measurement errors and performs better in terms of accuracy.[16] In Reference 16, for various failure conditions, a nontraditional filter that combines the UKF and singular value decomposition (SVD) approach is compared to its R-adaptive variant. For sensor problems, the SVD/UKF is utilized without any additional modifications. The filter's measurement noise covariance matrix is modified using a scale factor for the R-adaptive version (SVD/RUKF). As the vector measurements are first pre-processed in the SVD before executing the UKF and the R matrix for the UKF is autonomously set depending on the covariance for the SVD estimates, it is inferred that the nontraditional technique is intrinsically robust against sensor defects. Although the problem cannot be entirely fixed, its impact on the accuracy of attitude estimation is reduced. The SVD/UKF algorithm is more favorable, according to the results. In Reference 13, by testing with three pairs of process noises without any adaptation rules, the authors examined the filter's agility (how rapidly it reacts to changes in the environment), particularly while entering and exiting the eclipse. They did not, however, take into account faults of any kind or offer any guidelines for adaption.

The tuning of the filter in terms of the process noise covariance is one of the challenges for the non-traditional attitude filters that we encountered in prior investigations. A change in the process noise covariance of the filter results from variations in the disturbance torques, such as the residual magnetic torque, modeling errors in the satellite's dynamics, and any problem in the actuators. The nontraditional attitude filter, despite being robust to any variation in the measurements due to its nature, is unable to tune itself against variations in this type of process noise covariance.

When we utilize any of the conventional Kalman filtering methods, including the UKF,[17] for attitude estimation, they all share the same shortcoming: they are not resistant to environmental changes. If these changes occur, then the filter's estimation accuracy degrades, and if the faults persist for a long time, the filter may diverge. In space, extreme operating conditions and solar and magnetic field abnormalities are highly likely for any spacecraft. Due to this circumstance, we are looking for an adaptive UKF algorithm that we may use in a nontraditional attitude filter.

Since Mehra's earlier papers, a number of algorithms have been presented for proposing adaptive extensions to the Kalman filter.[18,19] Scaling the filter's covariance is one of these concepts. Different methods can be used to calculate the scaling parameters.[20–22] The UKF adaption can use this concept as well. In Reference 20, an adaptive Kalman filter is designed for the integrated navigation system, consisting of inertial and radar altimeters with an examination under the faulty measurements.[21] also proposes to use a measurement noise covariance adaptation in the filter by comparing single and multiple scale factors with an application on the unmanned aerial vehicles. In Reference 22, an adaptive Kalman filter is designed for the case of having interference on the global navigation satellite system measurements. These studies apply the filtering using the traditional approach on various systems but only considered adaptation in the measurement noise covariance and not in the process noise covariance.

In Reference 23, by properly adjusting the unscented transform parameters as well as the dynamic process model's process and measurement noise covariance matrices, the UKF's state estimation performance is enhanced. A basic model-based optimizer and a stochastic search technique are used to tackle the tuning problem. Because the optimization is done offline, the UKF is able to keep its low initial computational complexity. As a result, the numerical findings highlight how crucial it is to correctly tune the UKF parameters for the performance of the UKF state estimate.

In Reference 24, for the purpose of estimating pico-satellite attitude, the authors developed a RUKF method. The measurement noise covariance matrix of the UKF is tuned using a set of scale factors that are produced using the covariance matching method, which is the basis for the algorithm. A specific statistical function is used to first identify the measurement error, and then the estimated scale factors are used to strengthen the filter. In Reference 25, the results of this algorithm's testing for an EKF are compared to those of the UKF. In Reference 26, the approach is expanded for use in new measurement fault cases and a more challenging attitude estimation problem with quaternions. Lastly in Reference 27, the measurement and process noise covariance matrices of the UKF are modified by the authors' integrated approach for estimating satellite attitude. In all these studies,[24–27] for attitude estimation, the nontraditional method is applied.

The filtering problems in Kalman-based estimators using quaternions might be arose by limited computing power and storage space of the onboard microprocessor, process model uncertainties of environmental disturbances from inside and outside the satellite, quaternions normalization constraint. A multiplicative quaternion square root strong tracking estimator is proposed in Reference 28. The article proposes to use multiple fading factors to adjust process covariance matrix by giving more weight to sensor measurements than to corrupted state predictions caused by model uncertainties without considering a simultaneous covariance matching including the measurement corruptions as well. Similarly, in Reference 29, a Kalman-based estimator is presented that is robust against process model uncertainty, such as the initial errors, statistic errors of process noise, parameter mismatch and stochastic drifts but not robust against measurement faults at the same time. In Reference 30,31, two external covariance matching rules are designed using an online fault-detection method to determine whether it is necessary to update current noise covariance. If necessary, innovation-based method for process and residual-based method for measurements are used together but the type of fault (process or measurement) cannot be detected in this case. An adaptive UKF based on forgetting-factor-weight smoothing and multi-factor adaptation is proposed in Reference 32, by integrating the BeiDou Navigation Satellite System and the Inertial Navigation System (INS). This paper aims to improve the filtering performance in terms of computations and presents its results by comparing them with algorithms based on windowing and scale factors.

1.3 | Contributions of this study

In Reference 33, we extend our prior studies on nontraditional filtering and suggest an adaptation strategy for adjusting the filter's Q matrix. The SVD approach calculates the attitude of the nanosatellite using the magnetometer and Sun sensor measurements as the first stage of the algorithm, providing one estimate every frame. The Q-Adaptive UKF then receives these estimated attitude terms as input. In Reference 33, a method of adaptation based on just one fading element is proposed. The difference in the effects of the process noise covariance change on the estimation performance of each estimated state is the fundamental reason for using several fading factors. The influence of the process noise covariance change on each state should be carefully examined, especially for complicated multivariable systems, and instead of using a single component, a matrix made up of many fading factors should be utilized (such that it weights the adaptation differently for each state).

In this study the multiple fading factors-based adaptive singular value decomposition-aided unscented Kalman filter (SVD-aided UKF) for small satellite attitude estimation is proposed using quaternions as attitude representation. Constructing UKF using quaternions can be achieved by preserving the unity norm of the quaternions.[34] We first demonstrate the SVD-aided UKF approach's robustness to measurement noise increment defect. Furthermore, since the measurement model is made linear when the measurements are first processed using the SVD, we can easily change the Q matrix using a number of fading factors utilizing a covariance matching-based method. The adaptation of the Q matrix also gives us an algorithm that can simultaneously adapt the process and measurement noise covariance matrices, which is useful because the nontraditional attitude filtering algorithm is inherently adaptive against measurement faults of the noise-increment type in particular. Therefore, despite any change in the process and measurement noise covariance, the attitude and attitude rates of the satellite may still be determined with a desired accuracy. The aim of the paper is to estimate attitude with singularity-free quaternions using a simultaneously adaptive filter in terms of both process and measurement noises that is designed by having inherent R-adaptation and a Q-adaptation method with multiple fading factors. In summary, the significant contributions of this study can be listed as,

1. Linear measurements are utilized instead of conventional nonlinear measurements to simplify the design of the filtering step,
2. Instead of using an external rule, an inherent adaptation is incorporated into the filter for malfunction or faulty cases in measurements,
3. The divergence effect produced by arbitrary initial values is eliminated that may be significantly different from the correct values,
4. Reconfigurable filtering architecture is designed that is unaffected by sensor type or attitude measurement sequence,
5. Another adaptation rule for the process noise is proposed that works simultaneously with the measurement noise covariance adaptation,
6. The process noise covariance is adapted for each channel by defining multiple scaling.

The proposed adaptive SVD-aided UKF, which incorporates multiple fading factors, offers several benefits. One advantage is that it considers the impact of changes in process noise covariance on the estimation performance of each state variable. This is achieved by employing a matrix composed of multiple fading factors instead of relying on a single component. This approach is particularly valuable for complex systems with multiple variables. Another advantage is achieved by applying SVD to the measurements and linearizing the measurement model. By this way, we gain the flexibility to modify the Q matrix using multiple fading factors through a covariance matching-based technique. This adaptation of the Q matrix allows for the simultaneous adjustment of both the process and measurement noise covariance matrices. This capability is particularly valuable for the nontraditional attitude filtering algorithm, as it inherently adapts to measurement faults of the noise-increment type. Consequently, even in the presence of changes in the process and measurement noise covariance, the paper aims to accurately estimate the attitude and attitude rates of the satellite using singularity-free quaternions. This is achieved by employing a simultaneously adaptive filter that incorporates both process and measurement noise adaptation through inherent R-adaptation and a Q-adaptation method utilizing multiple fading factors.

In the following sections, we first describe the rotational motion of the satellite and the measurement models for the attitude sensors under the section of mathematical models. The attitude estimation algorithms are then given with the influence of process noise increment to the innovation. After giving details of the proposed estimation filter with simultaneous and multiple factor adaptation features, analyses and results are given. A summary and conclusion are finally given in the last section of the article.

2 | MATHEMATICAL MODELS

The mathematical models for the rotational motion of the satellite are presented including the rotational kinematics and rigid body dynamics. Then, the measurement models of the attitude sensors used in this study (i.e., magnetometer, sun sensor) are given.

2.1 | Rotational motion of the satellite

By using the quaternion attitude representation, the satellite's kinematics equation of motion can be expressed as follows[35]:

$$\dot{\boldsymbol{q}}(t) = \frac{1}{2}\Omega\left(\boldsymbol{\omega}_{BR}(t)\right)\boldsymbol{q}(t). \tag{1}$$

Here, $\boldsymbol{q}$ consists of four attitude parameters in the quaternion, $\boldsymbol{q} = \begin{bmatrix} q_1 & q_2 & q_3 & q_4 \end{bmatrix}^{\mathrm{T}}$. Since the last term is a scalar and the first three terms are vector terms, we may rewrite the quaternion as $\boldsymbol{q} = \begin{bmatrix} \mathbf{g}^{\mathrm{T}} & q_4 \end{bmatrix}^{\mathrm{T}}$ and $\mathbf{g} = \begin{bmatrix} q_1 & q_2 & q_3 \end{bmatrix}^{\mathrm{T}}$. In addition, the skew symmetric matrix $\Omega\left(\boldsymbol{\omega}_{BR}\right)$ is,

$$\Omega\left(\boldsymbol{\omega}_{BR}\right) = \begin{bmatrix} 0 & \omega_3 & -\omega_2 & \omega_1 \\ -\omega_3 & 0 & \omega_1 & \omega_2 \\ \omega_2 & -\omega_1 & 0 & \omega_3 \\ -\omega_1 & -\omega_2 & -\omega_3 & 0 \end{bmatrix}, \tag{2}$$

where ω_1, ω_2, and ω_3 are the components of $\boldsymbol{\omega}_{BR}$ vector which shows the body frame's angle of rotation with regard to the study's orbit frame, the reference frame. It is important to specify the body's angular rate vector in relation to the inertial axis frame independently from the angular velocity vector, $\boldsymbol{\omega}_{BI} = \begin{bmatrix} \omega_x & \omega_y & \omega_z \end{bmatrix}^{\mathrm{T}}$.$\boldsymbol{\omega}_{BI}$ and $\boldsymbol{\omega}_{BR}$ can be related via,

$$\boldsymbol{\omega}_{BR} = \boldsymbol{\omega}_{BI} - A\begin{bmatrix} 0 & -\omega_o & 0 \end{bmatrix}^{\mathrm{T}}. \tag{3}$$

Here, ω_o indicates the satellite's angular orbital velocity, which is calculated as $\omega_o = \left(\mu/r^3\right)^{1/2}$ assuming the satellite's orbit is circular. μ is the gravitational constant and r is the distance between the satellite's and Earth's centers of mass. In (3), A is the attitude matrix and the quaternions are connected to it by,

$$A = \left(q_4^2 - |\mathbf{g}|^2\right) I_{3\times3} + 2\mathbf{g}\mathbf{g}^T - 2q_4[\mathbf{g}\times], \tag{4}$$

where I_{3x3} is the identity matrix with the dimension of 3×3 and $[\mathbf{g}\times]$ is the skew-symmetric matrix given as follows:

$$[\mathbf{g}\times] = \begin{bmatrix} 0 & -g_3 & g_2 \\ g_3 & 0 & -g_1 \\ -g_2 & g_1 & 0 \end{bmatrix}. \tag{5}$$

We also require dynamic knowledge for a full-state attitude estimator where attitude and attitude rates are simultaneously computed. Based on Euler's equations, it is possible to deduce the satellite's dynamic equations:

$$J\frac{\boldsymbol{\omega}_{BI}}{dt} = \boldsymbol{N}_d - \boldsymbol{\omega}_{BI} \times \left(J\boldsymbol{\omega}_{BI}\right), \tag{6}$$

where J is the principal moments of inertia matrix as $J = \mathrm{diag}\left(J_x, J_y, J_z\right)$ and $\boldsymbol{N}_d$ is the vector of disturbance torque affecting the satellite. It should be noticed that the satellite's main axis of inertia are aligned with the body reference frame.

2.2 | Measurement models of the attitude sensors

In this paper, we outline our technique for a nanosatellite equipped with magnetometers and a sun sensor, two different types of attitude sensors. They are both classic examples of attitude sensors that provide unit vector measurements.[36] We require the unit vectors generated in the reference orbit frame that correspond to the unit vectors measured by the sensors in the spacecraft body frame in order to determine the attitude. The measurement models merely demonstrate the relationships between these computed and measured unit vectors in order to determine the attitude.

The IGRF model presented in is used to calculate the magnetic field vector in the regional geodetic North East Down (NED) frame.[37] The computed magnetic field vector must be converted to the orbital frame via a sequence of transformations because the orbital frame serves as the reference frame for attitude estimation. We need to be aware of the orbital parameters describing the satellite's position in order to do these operations. The satellite's position and the time data serve as the IGRF's inputs. The acquired magnetic field vector is normalized so that the algorithms can utilize it as a unit vector. It should be emphasized that in this case, we presume that one of the in-orbit or on-ground calibration techniques has already been used to calibrate the attitude sensors.[38,39] In light of this, the magnetometer measuring model can be described as follows:

$$\boldsymbol{B}_b = A\boldsymbol{B}_o + \eta_1. \tag{7}$$

Here, $\boldsymbol{B}_b$ is the measured magnetic field vector in the body frame, $\boldsymbol{B}_o$ is the calculated magnetic field vector in the orbit frame and η_1 is the assumed to be zero-mean Gaussian white noise in the magnetometer measurement noise.

The mathematical model presented in is applicable to the determination of the Sun direction in ECI (Earth-centered inertial) coordinates.[40] There is no need for the prior normalization procedure that was carried out for the magnetic field vector because it is directly acquired as a unit vector. However, the orbital coordinates are the reference system in the article. Therefore, using the satellite's orbital characteristics, the estimated Sun direction vector should be transformed into the orbital system. The measurement model can be expressed as follows while assuming that the Sun sensor is calibrated against any bias and/or misalignment:

$$\boldsymbol{S}_b = A\boldsymbol{S}_o + \eta_2. \tag{8}$$

Here, $\boldsymbol{S}_b$ is the measured Sun direction vector in the body frame, $\boldsymbol{S}_o$ is the calculated Sun direction vector in the orbit frame and η_2, which is taken to be zero-mean Gaussian white noise, is the measurement noise.

3 | SVD-AIDED UNSCENTED KALMAN FILTER (UKF) ALGORITHM FOR ATTITUDE ESTIMATION

The nontraditional attitude estimation procedure that is composed of two stages as SVD and UKF is presented in this section. The algorithm of SVD-aided UKF is named SaUKF for short throughout the text.

3.1 | SVD for attitude determination

Single-frame attitude estimate techniques include the SVD, q-method, QUEST, FOAM, and others.[36] Each one of them should reduce the loss function as specified in Reference 41. Due to its greater robustness, the SVD approach is chosen as the single-frame method in this instance.[36]

Given a set of $n \geq 2$ vector measurements, $\hat{u}_B^i$, in the body system, choosing to minimize the loss function given as for an ideal attitude matrix, A, is one possibility,

$$J(A) = \sum_{i=1}^{n} w_i \left| \hat{u}_B^i - A\hat{u}_R^i \right|^2, \tag{9}$$

where w_i is the weight of the ith vector measurement, $\hat{u}_R^i$ is the vector in the reference coordinate system.

When we express the loss function as (9), the problem reduces to the problem of maximizing the trace, $\mathrm{tr}\left(AB^T\right)$. Among the single-frame attitude estimate algorithms, the SVD is one of the most accurate, dependable, and robust techniques, as thoroughly addressed in Reference 36.

Decomposition of the matrix B into singular values,

$$B = U\sum^{\mathrm{T}} V^{\mathrm{T}} = U\mathrm{diag}\left[\sum_{11}\sum_{22}\sum_{33}\right]V^{\mathrm{T}}, \tag{10}$$

where U and V are orthogonal and the singular values obey $\sum_{11} \geq \sum_{22} \geq \sum_{33} \geq 0$. The trace is therefore maximized for,

$$U^T A_{opt} V = \mathrm{diag}\begin{bmatrix}1 & 1 & \det(U)\det(V)\end{bmatrix} \tag{11}$$

and the optimal rotation matrix is,

$$A_{opt} = U\mathrm{diag}\begin{bmatrix}1 & 1 & \det(U)\det(V)\end{bmatrix} V^{\mathrm{T}}. \tag{12}$$

By looking at the covariance matrix for rotation angle error, the accuracy of the estimated A_{opt} can be known. If we first define $s_1 = \sum_{11}$, $s_2 = \sum_{22}$, $s_3 = det(U)det(V)\sum_{33}$, then the covariance matrix P_{svd} is calculated as follows:

$$P_{svd} = U\mathrm{diag}\begin{bmatrix}(\mathrm{s}_2+\mathrm{s}_3)^{-1} & (\mathrm{s}_3+\mathrm{s}_1)^{-1} & (\mathrm{s}_1+\mathrm{s}_2)^{-1}\end{bmatrix} U^{\mathrm{T}}. \tag{13}$$

3.2 | UKF for attitude estimation

The unscented transform, a deterministic sampling approach we employ to get a minimal set of sample points (or sigma points) from the a priori mean and covariance of the states, is the foundation of the UKF. These sigma points are transformed nonlinearly. The altered sigma points are used to calculate the posterior mean and covariance.[26,42]

Since discrete-time nonlinear equations are used to construct the UKF, the following equations represent the process model:

$$x(k+1) = f(x(k), k) + w(k), \tag{14}$$

$$y(k) = Hx(k) + v(k). \tag{15}$$

Here, $x(k)$ is the state vector and $y(k)$ is the measurement vector. Moreover, $w(k)$ and $v(k)$ are the process and measurement error noises, which, according to the assumption, are processes with Gaussian white noise and a covariance of $Q(k)$ and $R(k)$, respectively, H is the measurement matrix of system. The UKF procedure is explained for the process given in (14) and (15) in the appendix section for brevity.

4 | INFLUENCE OF PROCESS NOISE INCREMENT TO THE FILTER'S INNOVATION

Let the measurements are processed by the UKF (A.1a) - (A.11b) and a process noise increment occurs at the iterations $k \geq \tau$. Process noise increment can be simulated by multiplying the process noise vector with the diagonal matrix $F(k)$, which diagonal elements meet the following condition: $\sigma_{ii}(k) \geq 1$, $(i = \overline{1,s})$ for $\forall k \geq \tau$ (s is the dimension of process noise vector). As it is clear, for the process noise change in the process channel j the appropriate diagonal element of $F(k)$ will be larger than 1, that is, $\sigma_{jj}(k) > 1$ for $\forall k \geq \tau$ and rest of the process channels become 1. Consequently, the diagonal elements of $F(k)$ can be presented in the following form:

$$\sigma_{ii} = \begin{cases} 1 : \text{no system noise change,} \\ > 1 : \text{system noise change.} \end{cases}$$

The mathematical model of process in this case can be written in the form:

$$x(k+1) = f(x(k), k) + F(k)w(k), \tag{16}$$

where

$$diag(F(k)) = \begin{cases} \begin{pmatrix} 1 & 1 & . & . & . & 1 \end{pmatrix} & \text{for } k < \tau, \\ \begin{pmatrix} \sigma_{11} & \sigma_{22} & . & . & . & \sigma_{ss} \end{pmatrix} & \text{if } \exists j \in (\overline{1,s}) \text{ where } \sigma_{jj} > 1 \text{ for } k \geq \tau. \end{cases} \tag{17}$$

Statement. The process noise increment leads to increment in the innovation covariance (A8).
Proof. The innovation covariance at the iteration steps $k \geq \tau$ can be expressed as follows:

$$\begin{aligned} P_{vv}(k+1|k) &= H(k+1)P(k+1/k)H^{\mathrm{T}}(k+1) + R(k+1) \\ &= H(k+1)\left[P^{*}(k+1|k) + F(k)Q(k)F^{\mathrm{T}}(k)\right]H^{\mathrm{T}}(k+1) + R(k+1). \end{aligned} \tag{18}$$

The theoretical innovation covariance increment is

$$\begin{aligned} \Delta P_{vv}(k+1/k) &= H(k+1)F(k)Q(k)F^{\mathrm{T}}(k)H^{\mathrm{T}}(k+1) - H(k+1)Q(k)H^{\mathrm{T}}(k+1) \\ &= H(k+1)\left[F(k)Q(k)F^{\mathrm{T}}(k) - Q(k)\right]H^{\mathrm{T}}(k+1). \end{aligned} \tag{19}$$

Since the matrices $F(k)$ and $Q(k)$ are assumed to be diagonal, the expression (19) can be rewritten in the following form:

$$\Delta P_{vv}(k+1/k) = H(k+1)\left[F^{2}(k)Q(k) - Q(k)\right]H^{\mathrm{T}}(k+1). \tag{20}$$

Since $Q(k)$ and $F(k)$ are positive-definite diagonal matrices and $F(k)$ has diagonal elements $\sigma_{ii}(k) \geq 1$, $(i = \overline{1,s})$ for $\forall k \geq \tau$, then the matrix $F^{2}(k)Q(k) - Q(k)$ is positive definite too. Taking into account that the system measurement matrix is the identity matrix $H(k+1) = I_{7\times 7}$, it follows that the matrix $H(k+1)\left[F^{2}(k)Q(k) - Q(k)\right]H^{T}(k+1)$ is positive definite. Since the innovation covariance increment is a positive-definite matrix; hence, the *Statement* above is true.

5 | Q-ADAPTIVE SVD-AIDED UKF ALGORITHM FOR ATTITUDE ESTIMATION

The SVD approach runs as the initial stage of the algorithm and provides one estimate per single frame for the nanosatellite attitude. The UKF is then provided with these estimated attitude terms as input. As a result, the satellite's attitude is calculated (see Figure 1). "SVD-aided UKF" is called "SaUKF" for short as mentioned earlier. "Q-Adaptive SVD-aided UKF" is called "ASaUKF" throughout the text for brevity.

The estimation covariance from the SVD is also input into the UKF method and used as the filter's measurement noise covariance matrix in addition to the estimated quaternions, that is, $R(k+1) = P_{svd}(k+1)$. Because of this, the nontraditional filter is intrinsically robust to measurement noise increments in particular. The SVD's estimation covariance, which is also the filter's measurement noise covariance, increases in the presence of a measurement error, allowing the filter to function without being significantly affected.

The adjustment of the filter's process noise covariance matrix, Q presents one challenge for nontraditional attitude filters.[43] When the environment changes, it is very important to optimize the process noise covariance. Any conditional change that might have an impact on the filter's process model is referred to here. These include adjustments to the inertia parameters (as when the satellite enters or exits an eclipse), adjustments to the disturbance torques, as well as adjustments to the controller parameters (such as a malfunction), though a controller is not covered in this work.

An adaptive technique is used to tweak the UKF's matrix in order to adapt it to the changing environment. The adaptation rule is comparable to a linear KF and simple to implement because the measurement model is linear.

Only when the actual values of the process noise covariance do not match the model employed in the filter's synthesis does the adaptive algorithm make the necessary corrections. Otherwise, the filter uses the standard algorithm (A.1a)–(A.11b) to operate.

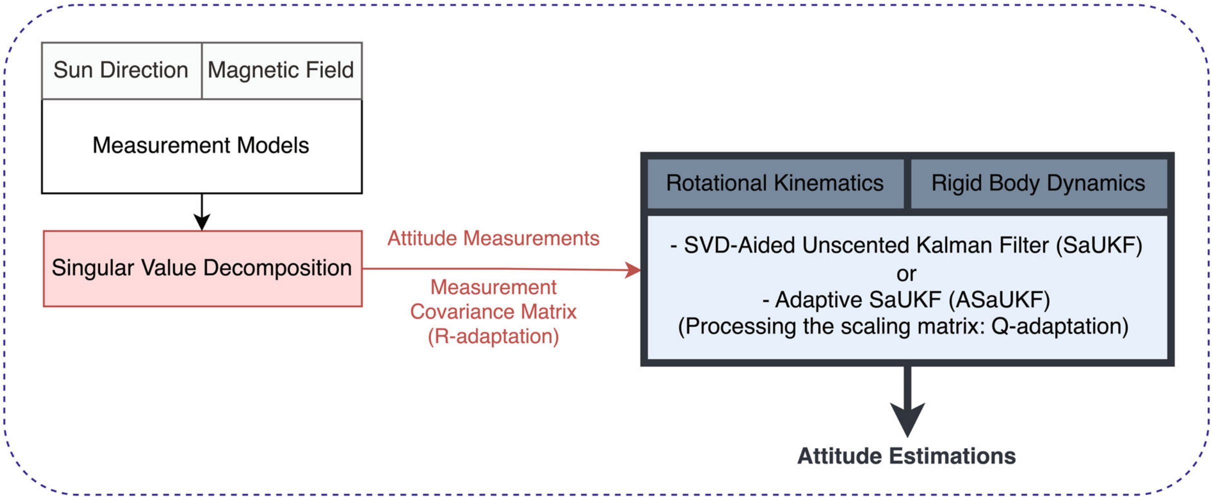

FIGURE 1 Flow chart of SaUKF and ASaUKF algorithms.

As seen from expressions (18) and (20), the noise increment type process noise change affects the innovation covariance of UKF. Therefore, the innovation covariance can be chosen as the monitoring statistic in the process noise covariance matching problem. The innovation covariance (18) at the iteration steps $k \geq \tau$ can be written as follows:

$$P_{vv}(k+1|k) = H(k+1)\left[P^{*}(k+1|k) + [F(k)]^{2}Q(k)\right]H^{T}(k+1) + R(k+1). \tag{21}$$

Substituting the adaptive scaling matrix $\Lambda(k) = [F(k)]^2$ into (21), we have

$$P_{vv}(k+1|k) = H(k+1)\left[P^{*}(k+1|k) + \Lambda(k)Q(k)\right]H^{\mathrm{T}}(k+1) + R(k+1) \tag{22}$$

or

$$P_{vv}(k+1|k) = H(k+1)P^{*}(k+1/k)H^{T}(k+1) + H(k+1)\Lambda(k)Q(k)H^{T}(k+1) + R(k+1) \tag{23}$$

The expression (23) represents the theoretical innovation covariance matrix that characterizes the accuracy of the innovation sequence known as a result of priori information. The real accuracy of the innovation sequence can be represented in terms of the sampling innovation covariance as follows:

$$P^{*}_{vv}(k+1|k) = \frac{1}{\mu}\sum_{j=k-\mu+1}^{k} v(j+1)v^{\mathrm{T}}(j+1), \quad (k \geq \mu). \tag{24}$$

Here, μ is the width of the moving window.

The expression for the adaptive scaling matrix $\Lambda(k)$ can be found from equalizing the theoretical and sample innovation covariance matrices,

$$\frac{1}{\mu}\sum_{j=k-\mu+1}^{k} v(j+1)v^{\mathrm{T}}(j+1) = H(k+1)P^{*}(k+1/k)H^{\mathrm{T}}(k+1) + H(k+1)\Lambda(k)Q(k)H^{\mathrm{T}}(k+1) + R(k+1). \tag{25}$$

It can be written from (25)

$$H(k+1)\Lambda(k)Q(k)H^{\mathrm{T}}(k+1) = P_{vv}(k+1|k) - H(k+1)P^{*}(k+1/k)H^{\mathrm{T}}(k+1) - R(k+1). \tag{26}$$

Multiplying by $H^T(k+1)$ on the left and by $H(k+1)$ on the right (26), then

$$\begin{aligned} &H^{\mathrm{T}}(k+1)H(k+1)\Lambda(k)Q(k)H^{\mathrm{T}}(k+1)H(k+1) = \\ &H^{\mathrm{T}}(k+1)\left[P_{vv}(k+1|k) - H(k+1)P^{*}(k+1/k)H^{\mathrm{T}}(k+1) - R(k+1)\right]H(k+1). \end{aligned} \tag{27}$$

In order to have the scaling matrix $\Lambda(k)$ on the left, let us multiply it by $\left[H^{\mathrm{T}}(k+1)H(k+1)\right]^{-1}$ on the left and by $\left[Q(k)H^{\mathrm{T}}(k+1)H(k+1)\right]^{-1}$ on the right. The equality is then expressed from the expression (27) as follows:

$$\Lambda(k) = \left[H^{\mathrm{T}}(k+1)H(k+1)\right]^{-1}H^{\mathrm{T}}(k+1)\left[P_{\nu\nu}(k+1|k) - H(k+1)P^{*}(k+1/k)H^{\mathrm{T}}(k+1) - R(k+1)\right] \times H(k+1)\left[Q(k)H^{\mathrm{T}}(k+1)H(k+1)\right]^{-1} \tag{28}$$

or by putting the innovation covariance $P_{\nu\nu}(k+1|k) = P^{*}_{\nu\nu}(k+1|k) = \frac{1}{\mu}\sum_{j=k-\mu+1}^{k} \nu(j+1)\nu^{\mathrm{T}}(j+1)$ into its place, Equation (28) becomes,

$$\Lambda(k) = \left[H^{\mathrm{T}}(k+1)H(k+1)\right]^{-1}H^{\mathrm{T}}(k+1) \times \left[\frac{1}{\mu}\sum_{j=k-\mu+1}^{k} \nu(j+1)\nu^{\mathrm{T}}(j+1) - H(k+1)P^{*}(k+1/k)H^{T}(k+1) - R(k+1)\right] \times H(k+1)\left[Q(k)H^{\mathrm{T}}(k+1)H(k+1)\right]^{-1}. \tag{29}$$

Here, $\mu$is the width of the moving window.

In a particular instance where all states are measured $(H(k+1) = I)$ as in case, (29) reduces to

$$\Lambda(k) = \left[\frac{1}{\mu}\sum_{j=k-\mu+1}^{k} \nu(j+1)\nu^{\mathrm{T}}(j+1) - P^{*}(k+1/k) - R(k+1)\right] Q^{-1}(k). \tag{30}$$

The primary distinction between the adaptive method and the existing adaptive UKF algorithms is that the adaptive algorithm is only employed when there are changes; otherwise, the procedure is conducted as efficiently as possible with a standard UKF. The checking of the process noise changes can be achieved using a statistical method presented in Reference 33.

6 | ANALYSIS AND RESULTS

A small satellite is considered for the analysis in order to test the presented algorithms. The simulation is realized for a tumbling satellite representing crucial measurement and environmental changes. The small satellite has the principal moment of inertia $J = \mathrm{diag}\begin{bmatrix}0.055 & 0.055 & 0.017\end{bmatrix}$ kg m^2. The algorithm runs for almost 1 orbital period with 1 Hz sampling rate for the filter and the sensors. The sensors are selected as three-axis magnetometers and three-axis Sun sensors corrupted by the standard deviations of $\sigma_B = 300$ nT for magnetometers and $\sigma_S = 0.002$ for Sun sensors. The initial state is $x_0 = \begin{bmatrix}0 & 0 & 0 & 1 & 0 & 0 & 0\end{bmatrix}$. The initial process noise covariance of the filters is $Q = \begin{bmatrix}10^{-4}I_{3\times3} & 0 \\ 0 & 10^{-9}I_{3\times3}\end{bmatrix}$. The design parameters for the satellite (mass-moment-of-inertia) and the sensors (three-axis magnetometer and coarse sun sensor corruptions) are selected by considering a nanosatellite. The parameters of the filtering stage are mostly designed as adaptive variables that are computed in the filter. The initial value of the process noise covariance is chosen arbitrarily, which then varies in time by using the defined adaptation rule. The measurement noise covariance, on the other hand, is directly obtained from SVD stage meaning that no arbitrarily chosen values is used. It should be remarked that this is done because arbitrary constant values in the filtering parameters that are chosen badly might corrupt the estimations.

Only when at least two measurements are available at the same time and the vectors are not parallel to one another can the single-frame attitude estimate methods be used. As a result, when the satellite is shadowed and two vectors are parallel, the single-frame technique is ineffective. To demonstrate how the filter behaves that is integrated with a single-frame method in these intervals, an eclipse period is introduced between the 500th and 1500th seconds.

The angle between the reference directions of sun and magnetic field lines are given in Figure 2. As can be seen, they become parallel at around 800th and 3400th seconds. As the first one is already under an eclipse period (zero-output for the sun sensors), only the second parallelism will be considered under parallel-vectors effect.

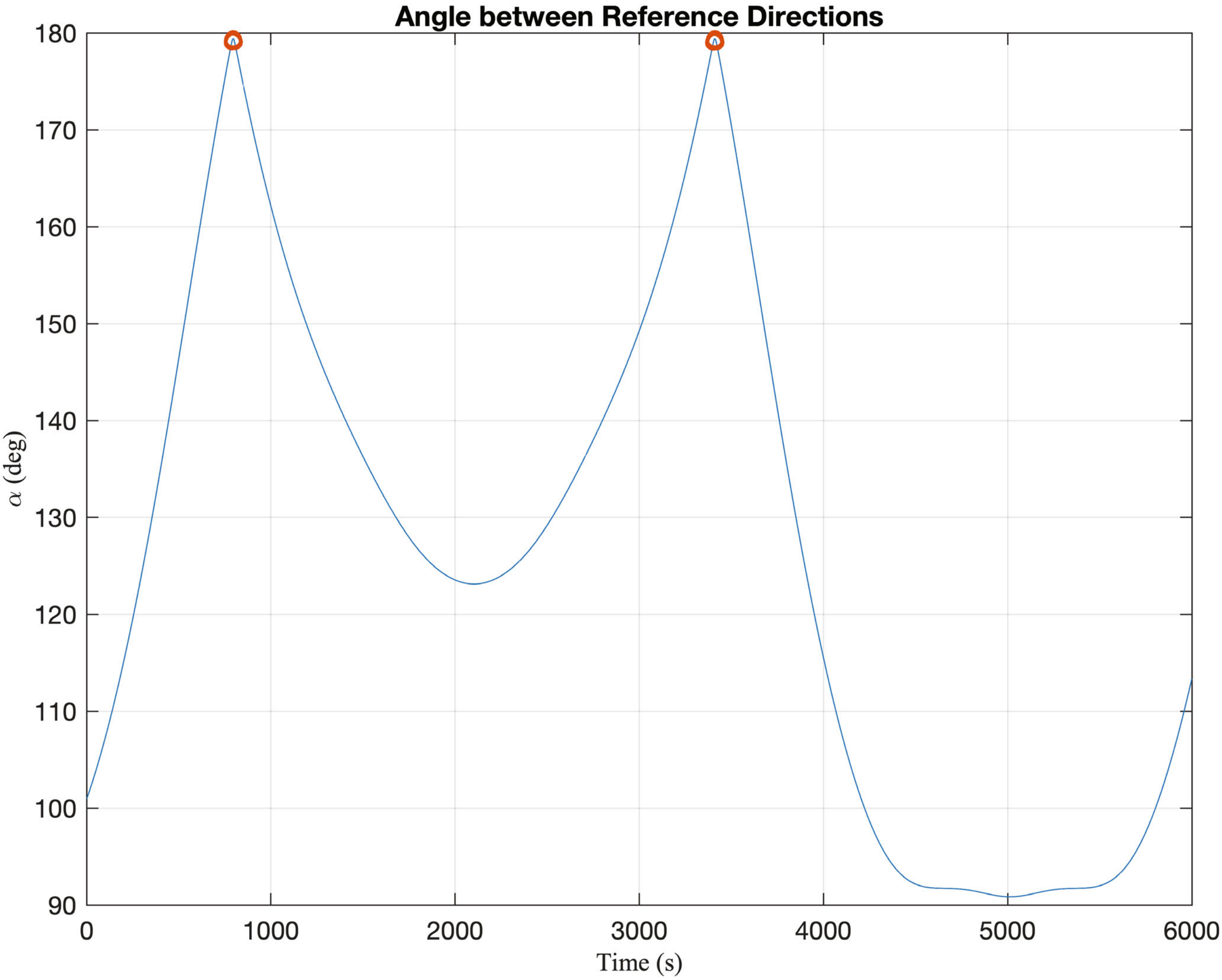

FIGURE 2 The angle between the reference directions (sun and magnetic field lines).

The SaUKF estimations of quaternions are given in Figure 3 under only eclipse and parallel vectors without any noise increment implementation. As can be seen, the estimations deteriorate in time during the eclipse (between two black lines) and parallel-vectors case at around the 3400th seconds. Here, the duration of the eclipse or parallelism is an important factor. When these periods are prolonged, the estimations tend to deteriorate progressively over time.

First section evaluates the SaUKF for the measurement faults between the 4500th and 5500th seconds. Second section evaluates the simultaneous adaptation for process noise increment in the same interval by comparing SaUKF and ASaUKF.

6.1 | Measurement noise increment case

For investigating the filter's ability to adapt against measurement faults the algorithm is tested for three different faults on the magnetometer measurements: low, medium and high noise increment for a short period of time. Measurement errors are identified by increasing the magnetometer measurements' standard deviation of noise by a fixed factor between 4500th and 5500th seconds. For the test case the constant term is selected as $\kappa = \{5 \quad 10 \quad 20\}$ to represent low, medium, and high increment cases.

$$B_b(k) = A(k)\boldsymbol{B}_o(k) + \eta_1(k) \times \kappa, \quad (4500 \leq k \leq 5500) \tag{31}$$

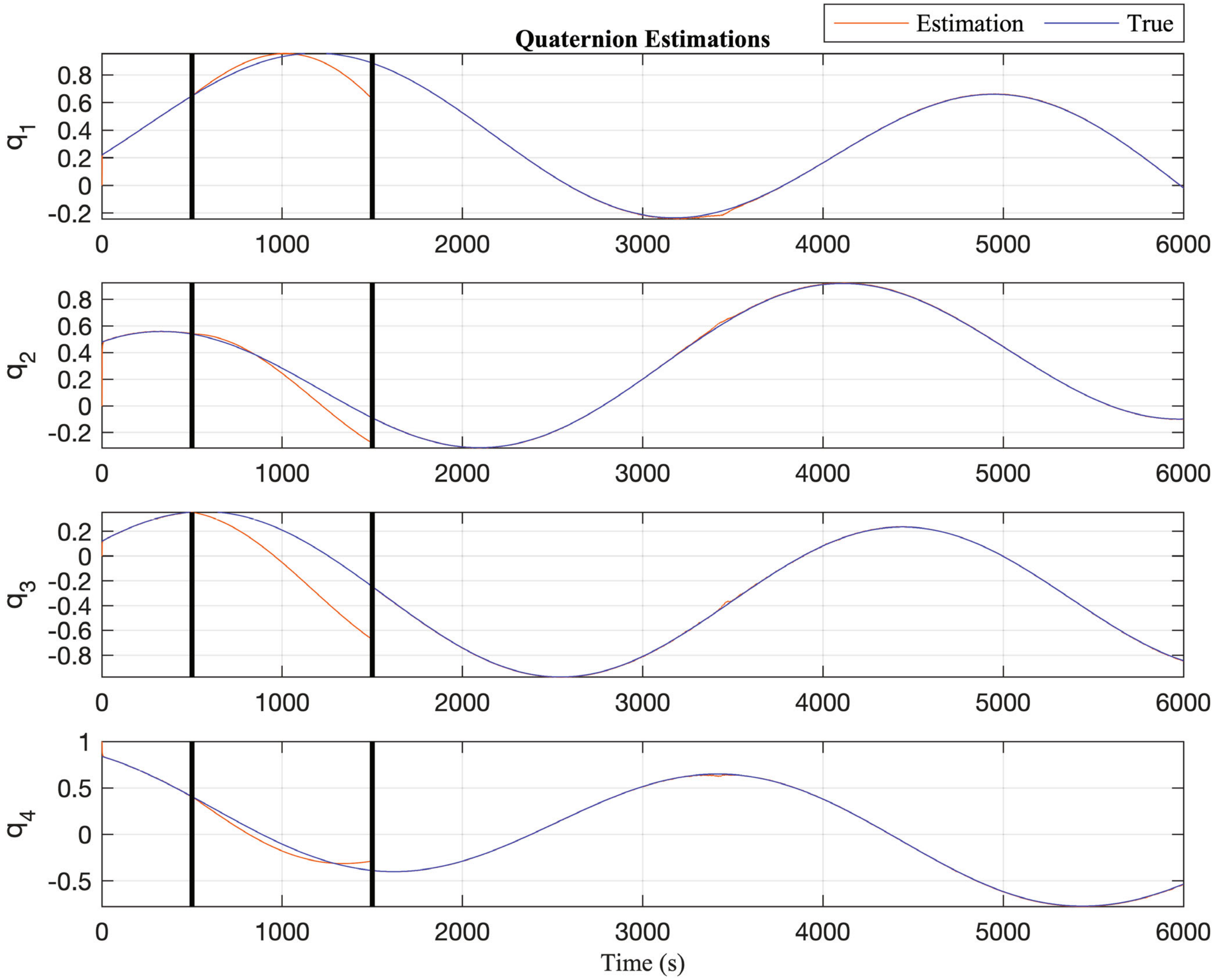

FIGURE 3 The quaternion estimations without any noise increment on the measurement or process.

In Figure 4, quaternion estimations of SaUKF are presented when having noise increments of low, medium and high levels, respectively. Here, R matrix's diagonal elements varies by adjusting the noise's level to account for its increase between the 4500th and 5500th s. In Figure 4A, a low-level increment is introduced in the magnetometer measurements, which had minimal impact on both the SVD measurements and the SaUKF estimations. The medium noise increment in Figure 4B affected the estimations to a similar extent as the parallelism affected the outputs. However, the estimations were impacted even more significantly with a high noise increment in Figure 4C, as anticipated. Nevertheless, the quaternions were still reasonably well estimated despite these challenges. An external adaptation rule for making the filter robust against measurement faults could also be defined for such a case, which would make harder to define simultaneous adaptation in the process. So, a similar behavior is obtained by the inherent adaptation rule of SVD directly. By this way, SaUKF is designed with R-adaptive structure without a need of externally defined adaptation rule as presented in Figure 5. The measurement covariance matrix diagonal elements in case of no fault are presented in Figure 5A. The differences in the elements for three levels of increment are presented in Figure 5B. Each panel of Figure 5B is composed by subtracting the no fault case measurement noise covariance matrix's diagonal elements from the high, medium and low-level noise increment cases. Even though it cannot remove the fault completely attitude quaternions can be estimated reasonably well. The outputs for each case are shown in a complementary table (Table 1). The estimation errors from low to medium levels of increment (i.e., twice of the low increment) show themselves as double amount of error. Same applies from medium to high level of increment.

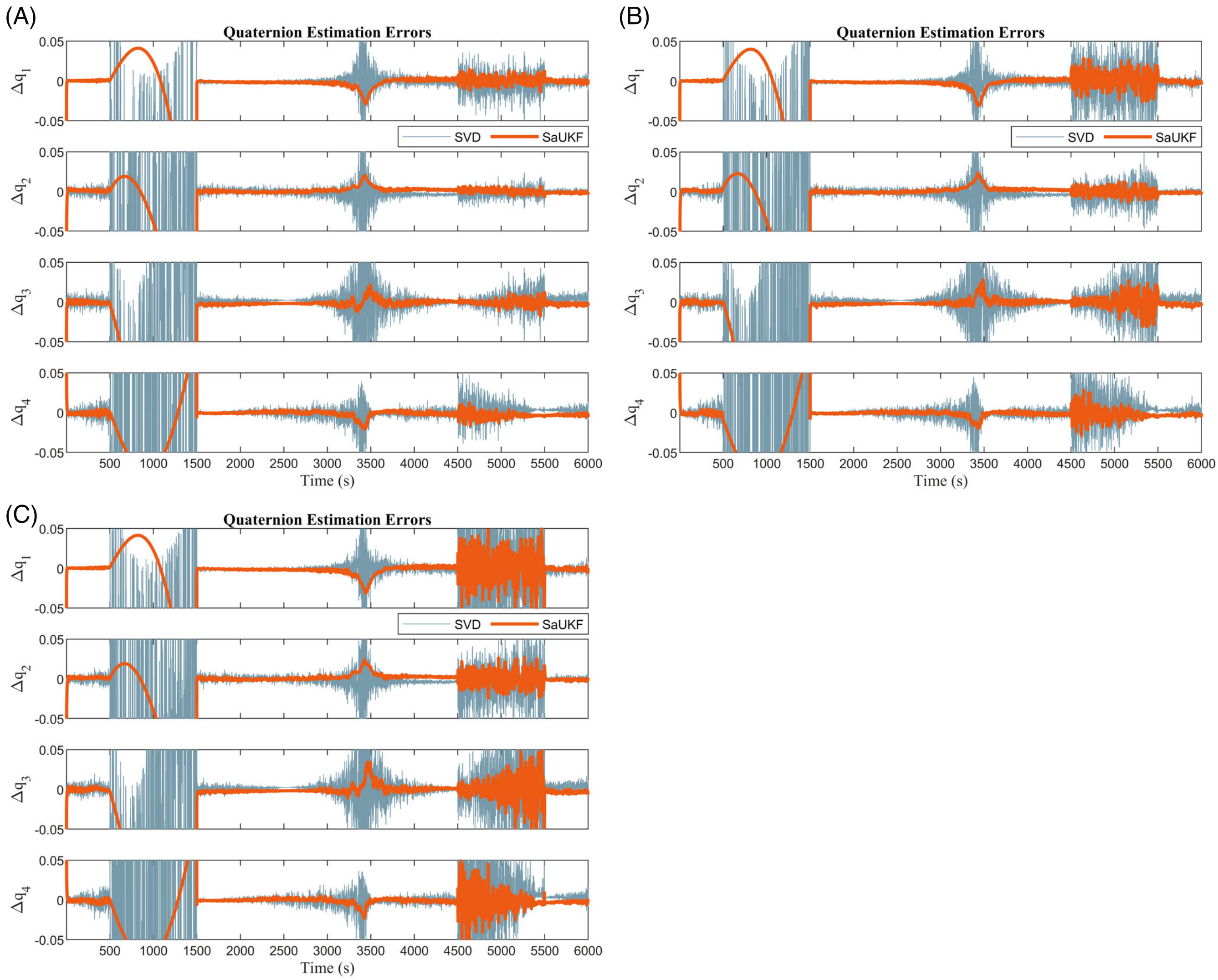

FIGURE 4 Quaternion estimation errors of SaUKF algorithm under magnetometer measurement noise increment applied as κ_{low} (A), κ_{medium} (B), and κ_{high} (C).

Remark that the obtained attitude terms by SVD method are aided to the Kalman filtering as input measurements. In addition to the determined attitude, the SVD's attitude covariance, which is calculated at each iteration step, is also fed into the algorithm and used as the filter's measurement noise covariance matrix making the filter inherently robust against the noise increment type of faults on the measurements.

6.2 | Process noise increment case

The (inherent) R adaptation of the SaUKF is investigated for measurements under low, medium and high noise increment cases. Here, we show that the nontraditional attitude filter can be R and Q adaptive simultaneously. Similarly, with the previous section, eclipse period is from 500th s to 1500th s. The process noise is increased as $Q = \begin{bmatrix} 10^{-4}\mathrm{diag}\left(\mathrm{K}_{1x3}\right) & 0_{3x3} \\ 0_{3x3} & 10^{-9}\mathrm{diag}\left(\mathrm{K}_{1x3}\right) \end{bmatrix}$ between the 4500th and 5500th seconds to simulate the effects of model uncertainties caused by environment changes and evaluate the effectiveness of the proposed Q-adaptation algorithm for the attitude filter by applying the constant increment vectors of $\mathrm{K}_{\mathrm{low}} = \left\{10^2 \quad 2\times10^2 \quad 2\times10^3\right\}$, $\mathrm{K}_{\mathrm{medium}} = \left\{10^3 \quad 2\times10^3 \quad 2\times10^4\right\}$, and $\mathrm{K}_{\mathrm{high}} = \left\{10^4 \quad 2\times10^4 \quad 2\times10^4\right\}$ for each channel of attitude and angular rates. As we use

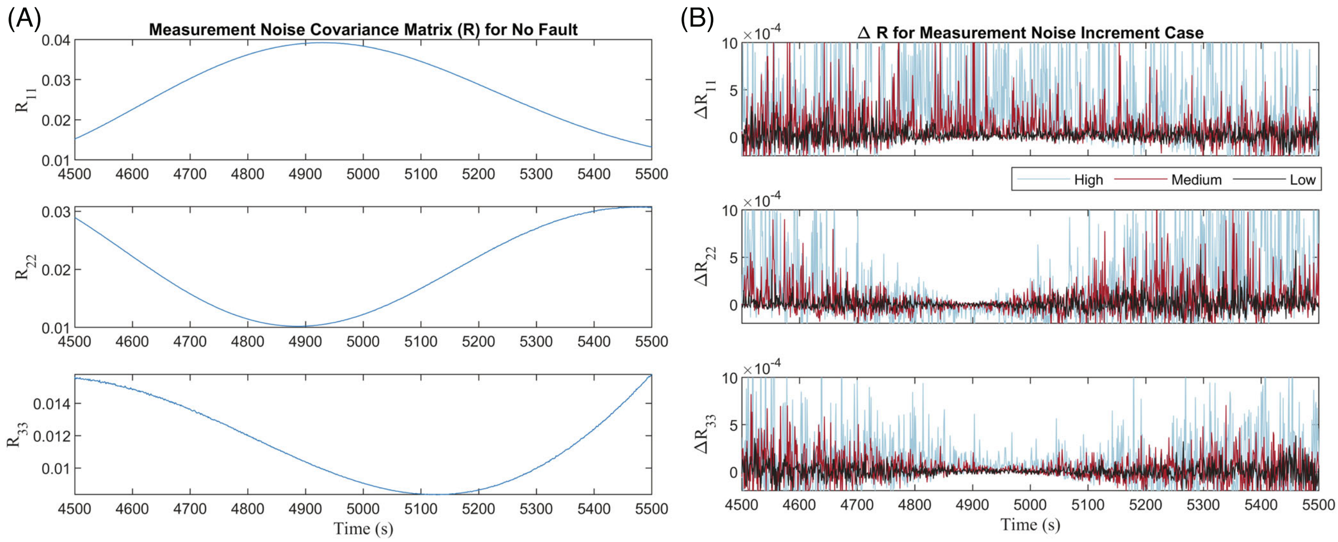

FIGURE 5 (A) Measurement noise covariance matrix (R) diagonals in case of no fault on the measurements. (B) Differences in the diagonals for different noise increment cases as κ_{low}, κ_{medium}, and κ_{high}.

TABLE 1 RMS error for SaUKF for measurement noise increment case.

RMS Error	Measurement noise increment		
	κ_{low}	κ_{medium}	κ_{high}
q_1	0.00481	0.00946	0.01798
q_2	0.00253	0.00441	0.00860
q_3	0.00378	0.00778	0.01458
q_4	0.00520	0.00723	0.01362

multiple measurement noise scaling factors aka adaptive factors, having different increments on each channel will result in having different factors for each channel of the factor.

Quaternion estimation errors of ASaUKF are presented in Figure 6. The subfigures (A), (B), and (C) show the cases of having low, medium, and high process noise increments. The difference between the low, medium, and high process noise levels cannot be distinguished by looking at the subfigures. There are three periods seen on the figure that are not estimated as accurately as the rest of the time. One is the eclipse period between 500 and 1500 s. This interval can be managed by switching to magnetometer-based estimation filter. Same applies for the second interval of having parallel vectors of sun and magnetic field directions around the 3400th second. Third interval is the noisy interval of process covariance between 4500 and 5500 s. This is the period that we would like to have a close look. In order to compare the filter that uses a process noise adaptation rule with the filter that does not have it, the RMS errors for this interval is given in Table 2 for each filter for each scenario. The estimations of SaUKF does not have an adaptive structure in terms of process noise covariance. Therefore, the estimation errors increase from low to high increment cases for SaUKF whereas the estimation errors of ASaUKF do not vary much. This is a clear output of achieving a successful adaptation in process covariance for each channel. This adaptation is performed using the adaptation factors presented in Figure 7 for each case. Please be careful in reading this figure as it has different scaling in the y-axes for better view of the changes in the factors. From this, we can state that during each process noise increment, ASaUKF is more reliable than SaUKF even though we still experience deterioration in the attitude estimations.

For giving more clear understanding of Table 2, Figure 8 is presented for various process noise increments. The increment values (K) are given the same for every channel as $Q = \mathrm{K}\begin{bmatrix} 10^{-4}\mathrm{I}_{3x3} & 0_{3x3} \\ 0_{3x3} & 10^{-9}\mathrm{I}_{3x3} \end{bmatrix}$. The increment data set varies

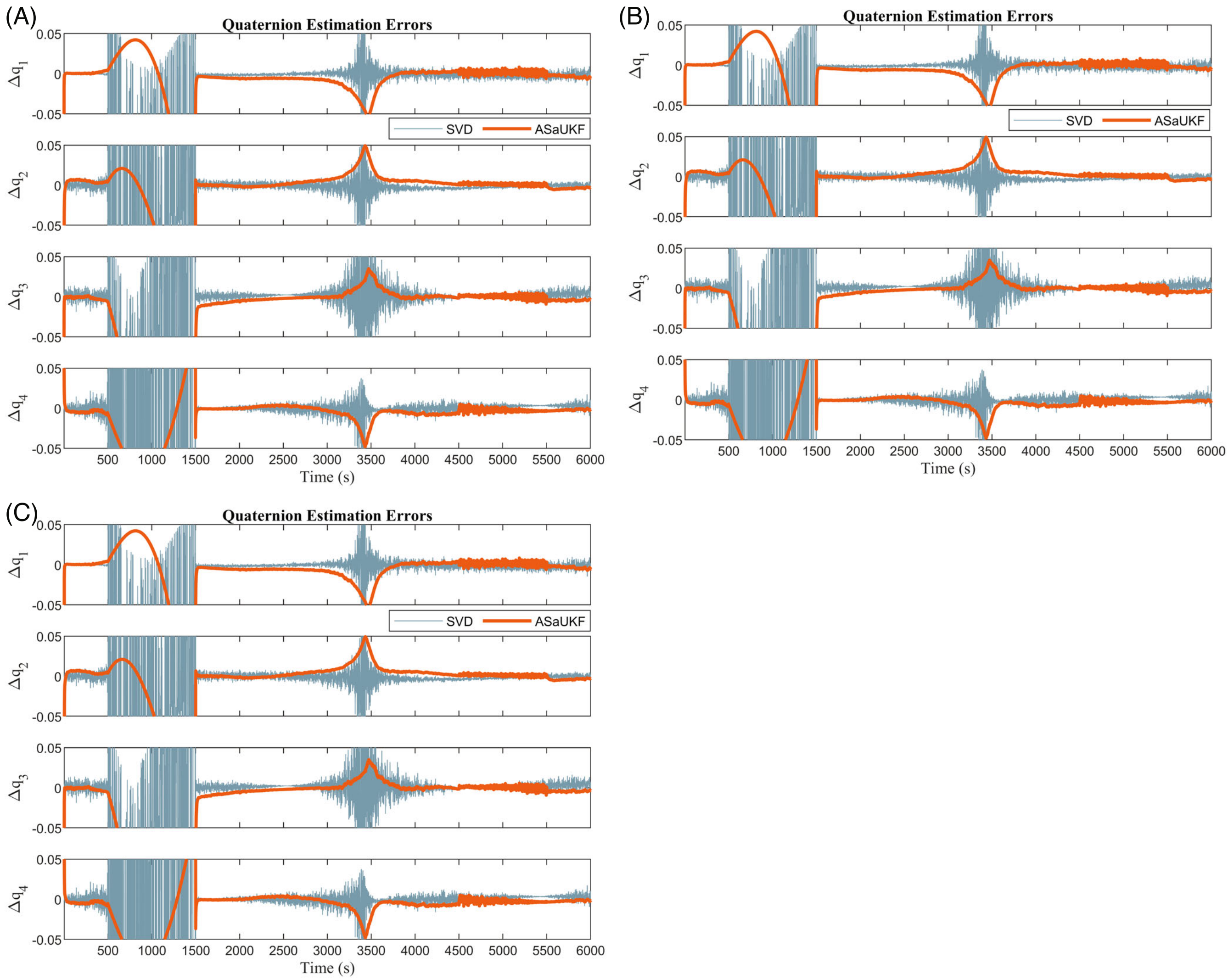

FIGURE 6 Quaternion estimation errors of ASaUKF algorithm under process noise increment applied as K_{low} (A), K_{medium} (B), and K_{high} (C).

TABLE 2 RMS error for SaUKF and ASaUKF for process noise increment case.

RMS Error	Process noise increment					
	K_{low}		K_{medium}		K_{high}	
	SaUKF	ASaUKF	SaUKF	ASaUKF	SaUKF	ASaUKF
q_1	0.00237	0.00275	0.00301	0.00274	0.00327	0.00274
q_2	0.00170	0.00161	0.00183	0.00162	0.00188	0.00162
q_3	0.00198	0.00188	0.00221	0.00188	0.00241	0.00188
q_4	0.00299	0.00296	0.00305	0.00296	0.00321	0.00296

from 10^3 to 8×10^4 given between 4500- and 5500-second interval as demonstrated in this section. RMS errors are calculated for this period of time at each case. This means that each data point in the figure corresponds to the RMS error obtained from a complete run of an orbital period. The trend of the estimation errors for each filter can be clearly seen. It can be seen that the SaUKF has a rapid increase in the estimation errors for this kind of uncertainty that might be caused by the environmental changes. ASaUKF, on the other hand, moderately increases by the given increment. ASaUKF is not affected by the process noise increments especially at the beginning, and stay at the same error level whereas the SaUKF has a leap in that interval and increases slowly afterwards. Here, it needs to be remarked that the proposed ASaUKF is

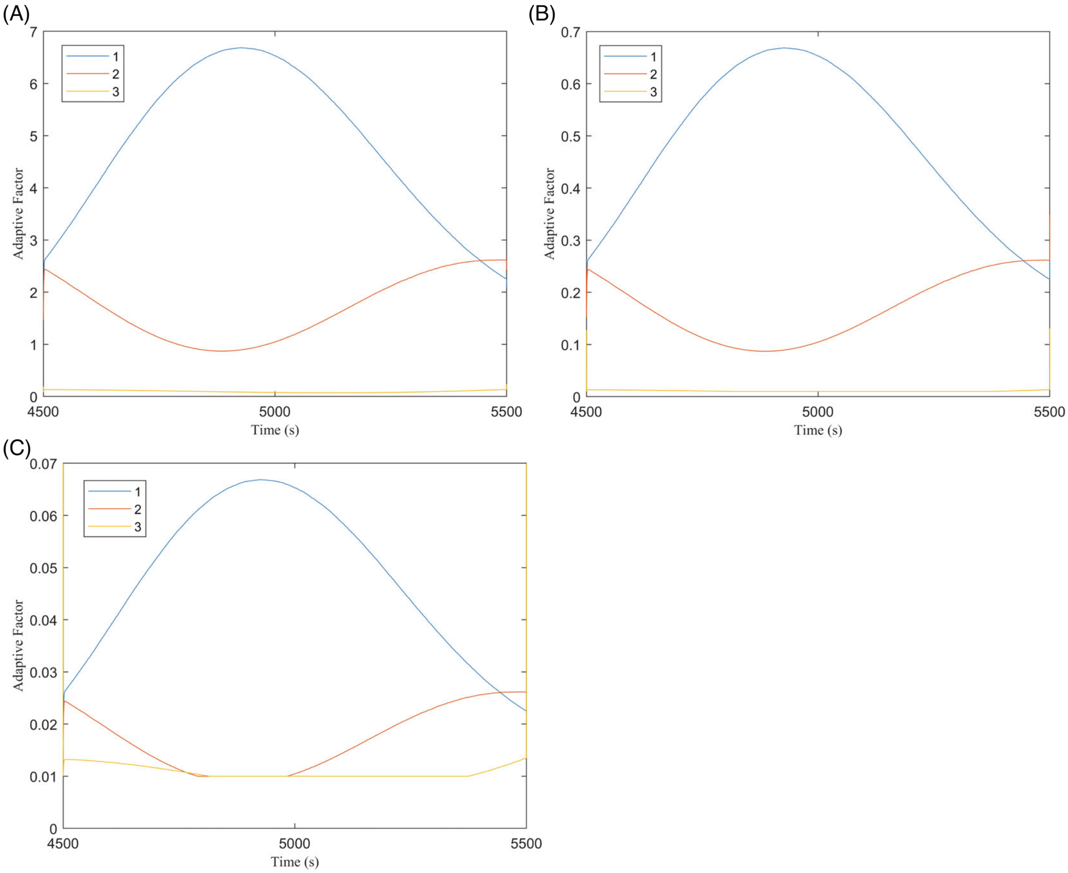

FIGURE 7 Adaptive factors for each channel of ASaUKF algorithm under process noise increment applied as K_{low} (A), K_{medium} (B), and K_{high} (C).

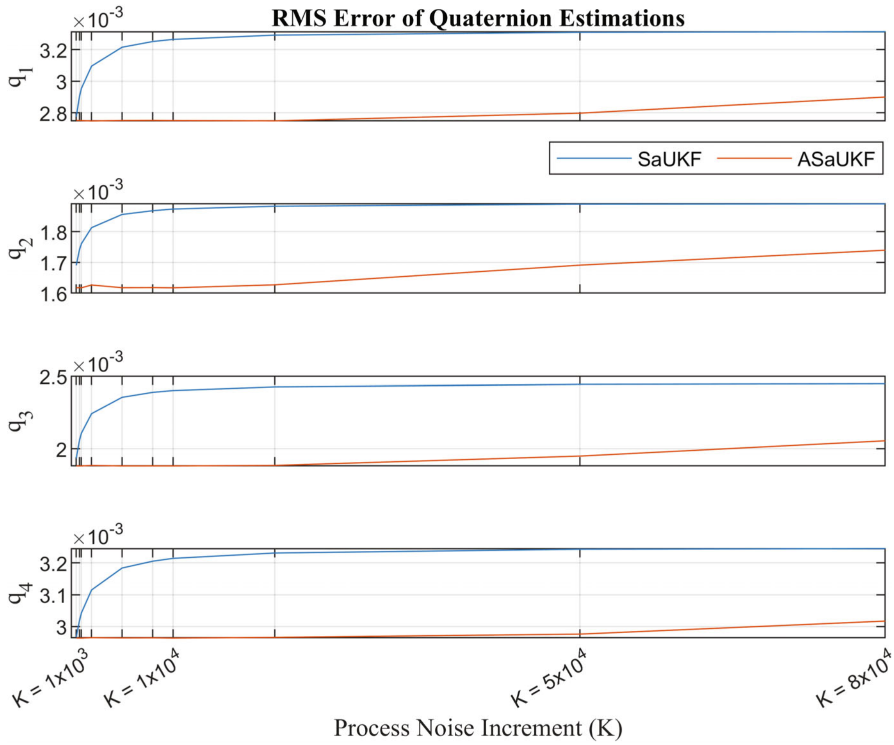

FIGURE 8 RMS Errors of SaUKF and ASaUKF algorithms under various process noise increments applied by the term K same for each channel.

robust against initialization errors, system noise uncertainties, and measurement noise uncertainties altogether by having two adaptations at the same time.

7 | CONCLUSIONS

In this paper, an attitude filtering technique is proposed that simultaneously adapts the process and measurement noise covariance matrices. To begin with, the unscented Kalman filter (UKF) and SVD methods are combined to estimate a nanosatellite's attitude. As measurement inputs for the UKF, the quaternion measurements from the SVD algorithm are utilized, and the measurement noise covariance matrix is taken to be the same as the SVD's estimation covariance for the attitude estimation error. In contrast to the conventional filters that employ the available vector data directly, this method of attitude filtering that processes the measurements under a single-frame method is called nontraditional attitude filtering.

For the purpose of estimating a nanosatellite's attitude, simulations are compared using the (process) adaptive and non-adaptive versions of the nontraditional attitude filter. The SVD-aided UKF (SaUKF) algorithm is inherently robust against measurement faults. Various levels of noise-increment type measurement faults are tested. In order to modify its R-matrix, UKF employs the SVD's estimation covariance as the measurement noise covariance. In the case of process noise increment, the multiple fading factors based adaptive SVD-aided UKF (ASaUKF) can adapt to the changing environment better than the SaUKF. The simultaneous adaptation of the filter is tested under a comprehensive analysis of process noise increments. In contrast to the SaUKF, which jumps throughout that time, the ASaUKF maintains nearly the same error level and is almost unaffected by the process noise increases. As a shortcoming, even the proposed ASaUKF is unaffected by the process noise uncertainties at the beginning unlike SaUKF, after a level of noise increment the proposed method does start to be affected as well. Therefore, the critical level of uncertainty needs to be addressed for a specific application of interest. For our case, the filter started to be affected after incrementing the process noise by about 20,000 times, which is expected to be improbable for space missions. Another disadvantage is using it only if two or more vector observations are available. Otherwise, the estimations might deteriorate in time. To realize the proposed ASaUKF, the innovation vectors must be known for μ measurement data (μ is the width of the moving window) and that causes an increment in the storage burden, as well as the requirement to know the width of the moving window (the window size μ is chosen empirically since there is no theoretically justified choice for the number μ). Besides, in order to estimate covariance matrix of the process noise based on the innovation, number, type and distribution of measurements must be consistent for all data within a window.

For the future studies, uncertainties in process noise mean can be examined after a careful theoretical proof process for the influences of the bias type process noise uncertainties to the innovation of SVD-Aided UKF.

DATA AVAILABILITY STATEMENT

The data that support the findings of this study are available from the corresponding author upon reasonable request.

ORCID

Chingiz Hajiyev https://orcid.org/0000-0003-4115-341X
Demet Cilden-Guler https://orcid.org/0000-0002-3924-5422

REFERENCES

1. Sekhavat P, Gong Q, Ross IM. NPSAT 1 parameter estimation using unscented Kalman filter. *Proc 2007 Amer Control Conf*. 2007;4445-4451. doi:10.1109/ACC.2007.4283031
2. Soken HE, Hajiyev C. Estimation of Pico satellite attitude dynamics and external torques via unscented Kalman filter. *J Aerospace Technol Manage*. 2014;6(2):149-157.
3. Springmann JC, Cutler JW. Flight results of a low-cost attitude determination systems. *Acta Astronaut*. 2014;99:201-214.
4. Vinther K, Jensen KF, Larsen JA, Wisniewski R. Inexpensive Cubesat attitude estimation using quaternions and unscented Kalman filtering. *Autom Control Aerosp*. 2011;4(1).
5. Söken HE, Hajiyev C. Estimation of Pico satellite attitude dynamics and external torques via unscented Kalman filter. *J Aerosp Technol Manage*. 2014;6(2):149-157.
6. Lee DY, Par H, Romano M, Cutler J. Development and experimental validation of a multi-algorithmic hybrid attitude determination and control system for a small satellite. *Aerosp Sci Technol*. 2018;78:494-509.

7. Habib TMA. A comparative study of spacecraft attitude determination and estimation algorithms (a cost–benefit approach). *Aerosp Sci Technol*. 2013;26(1):211-215.
8. Zagorski P, Dziwinski T, Tutaj A. Steepest Descent Quaternion Attitude Estimator. *Aerosp Sci Technol*. 2018;77:1-10.
9. Hajiyev C, Bahar M. Attitude determination and control system design of the ITU-UUBF LEO1 satellite. *Acta Astronaut*. 2003;52(2–6):493-499.
10. Mimasu BY, Van der Ha JC. Attitude determination concept for QSAT. *Trans Japan Soc Aeronaut Space Sci: AerospTechnol Japan*. 2009;7:63-68.
11. Hajiyev C, Cilden D, Somov Y. Gyro-free attitude and rate estimation for a small satellite using SVD and EKF. *Aerosp Sci Technol*. 2016;55:324-331.
12. Hajiyev C, Cilden-Guler D. Review on Gyroless attitude determination methods for small satellites. *Prog Aerosp Sci*. 2017;90:54-66.
13. Cilden D, Soken HE, Hajiyev C. Nanosatellite attitude estimation from vector measurements using SVD-AIDED UKF algorithm. *Metrol Measur Syst*. 2017;24(1):113-125.
14. Soken HE, Cilden D, Hajiyev C. Attitude estimation for nanosatellites using singular value decomposition and unscented Kalman filter. International Symposium on Space Technology and Science (ISTS). 2015.
15. Cilden D, Hajiyev C, Soken HE. Attitude and attitude rate estimation for a nanosatellite using SVD and UKF. *7th Int Conf Recent Adv Space Technol*. 2015;695-700. doi:10.1109/RAST.2015.7208431
16. Cilden-Guler D, Soken HE, Hajiyev C. Non-traditional robust UKF against attitude sensors faults. *31st International Symposium on Space Technology and Science (ISTS)*, d-077. 2017.
17. Julier SJ, Uhlmann JK, Durrant-Whyte HF. A new approach for filtering nonlinear systems. *Amer Control Conf*. 1995;3:1628-1632.
18. Mehra RK. On the identification of variances and adaptive filtering. *IEEE Trans Automat Contr*. 1970;15(2):175-184.
19. Mehra R. Approaches to adaptive filtering. *IEEE Trans Automat Contr*. 1972;17(5):693-698.
20. Hajiyev C. Adaptive filtration algorithm with the filter gain correction applied to integrated INS/radar altimeter. *Proc Instit Mech, G: J Aerosp Eng*. 2007;221(5):847-885.
21. Hajiyev C, Soken HE. Robust estimation of UAV dynamics in the presence of measurement faults. *J Aerosp Eng*. 2012;25(1): 80-89.
22. Kang CH, Kim SY, Park CG. A GNSS interference identification and tracking based on adaptive fading Kalman filter. *IFAC Proc Vol*. 2014;47(3):3250-3255.
23. Scardua LA, da Cruz JJ. Complete offline tuning of the unscented Kalman filter. *Automatica*. 2017;80:54-61.
24. Soken HE, Hajiyev C. Pico satellite attitude estimation via robust unscented Kalman filter in the presence of measurement faults. *ISA Trans, J Autom Measur*. 2010;49(3):249-256.
25. Soken HE, Hajiyev C. REKF and RUKF for Pico satellite attitude estimation in the presence of measurement faults. *J Syst Eng Electron*. 2014;25(2):288-297.
26. Soken HE, Hajiyev C, Sakai S. Robust Kalman filtering for small satellite attitude estimation in the presence of measurement faults. *Eur J Control*. 2014;20(2):64-72.
27. Hajiyev C, Soken HE. Robust adaptive unscented Kalman filter for attitude estimation of Pico satellites. *Int J Adapt Control Signal Process*. 2014;28(2):107-120.
28. Ma H, Zhang X, Lu Z, Liao W. An improved central difference Kalman filter for satellite attitude estimation with state mutation. *Int J Robust Nonlinear Control*. 2022;32(6):3442-3468.
29. Hu G, Gao S, Zhong Y, Gao B, Subic A. Modified strong tracking unscented Kalman filter for nonlinear state estimation with process model uncertainty. *Int J Adapt Control Signal Process*. 2015;29(12):1561-1577.
30. Zheng B, Fu P, Li B, Yuan X. A robust adaptive unscented Kalman filter for nonlinear estimation with uncertain noise covariance. *Sensors*. 2018;18(3):808.
31. Zhang Z, Zheng L, Li Y, Wu H, Liang Y, Qiao X. Correction adaptive square-root cubature Kalman filter with application to autonomous vehicle target tracking. *Meas Sci Technol*. 2021;32(11):115101.
32. Sun J, Tao L, Niu Z, Zhu B. An improved adaptive unscented Kalman filter with application in the deeply integrated BDS/INS navigation system. *IEEE Access*. 2020;8:95321-95332.
33. Hajiyev C, Soken HE, Cilden-Guler D. Nontraditional attitude filtering with simultaneous process and measurement covariance adaptation. *J Aerosp Eng*. 2019;32(5):4019054.
34. Menegaz HMT, Ishihara JY. Unscented and square-root unscented Kalman filters for quaternionic systems. *Int J Robust Nonlinear Control*. 2018;28(15):4500-4527.
35. Wertz JR. *Spacecraft Attitude Determination and Control*. Kluwer Academic Publishers; 1988.
36. Markley FL, Mortari D. Quaternion attitude estimation using vector observations. *J Astronaut Sci*. 2000;48(2):359-380.
37. Alken P, Thébault E, Beggan CD, et al. International geomagnetic reference field: the thirteenth generation. *Earth, Planets and Space*. 2021;73(49). doi:10.1186/s40623-020-01288-x
38. Alonso R, Shuster MD. Complete linear attitude-independent magnetometer calibration. *J Astronaut Sci*. 2002;50:477-490.
39. Soken HE, Hajiyev C. UKF-based reconfigurable attitude parameters estimation and magnetometer calibration. *IEEE Trans Aerosp Electron Syst Trans Aerosp Electron Syst*. 2012;48(3):2614-2627.
40. Vallado DA. *Fundamentals of Astrodynamics and Applications*. 3rd ed. Microcosm Press/Springer; 2007.
41. Wahba G. Problem 65-1: a least squares estimate of satellite attitude. *Soc Indus Appl Math Rev*. 1965;7(3):409.

42. Julier SJ, Uhlmann JK, Durrant-Whyte HF. A new method for the nonlinear transformation of means and Covariances in filters and estimators. *IEEE Trans Automat Contr*. 2000;45(3):477-482.
43. Hajiyev C, Soken HE, Cilden-Guler D. Q-adaptation of SVD-aided UKF algorithm for nanosatellite attitude estimation. *IFAC–Pap OnLine*. 2017;50(1):8273-8278.

How to cite this article: Hajiyev C, Cilden-Guler D. Attitude filtering with uncertain process and measurement noise covariance using SVD-aided adaptive UKF. *Int J Robust Nonlinear Control*. 2023;33(17):10512-10531. doi: 10.1002/rnc.6896

APPENDIX A

The UKF algorithm's first phase is deciding the $2n + 1$ sigma points with a mean of $\hat{x}(k|k)$ and a covariance of $P(k|k)$. For an n dimensional state vector, these sigma points are obtained by,

$$\boldsymbol{x}_0(k|k) = \hat{\boldsymbol{x}}(k|k), \tag{A.1a}$$

$$\boldsymbol{x}_\gamma(k|k) = \hat{\boldsymbol{x}}(k|k) + \left(\sqrt{(n+\kappa)P(k|k)}\right)_\gamma, \tag{A.1b}$$

$$\boldsymbol{x}_{\gamma+n}(k|k) = \hat{\boldsymbol{x}}(k|k) - \left(\sqrt{(n+\kappa)P(k|k)}\right)_\gamma, \tag{A.1c}$$

where $\boldsymbol{x}_0(k|k)$, $\boldsymbol{x}_\gamma(k|k)$, and $\boldsymbol{x}_{\gamma+n}(k|k)$ are sigma points, n is the state number, and κ is the scaling parameter which is employed for fine tuning. $\left(\sqrt{(n+\kappa)P(k|k)}\right)_\gamma$ corresponds to the γ^{th} column of the indicated matrix and γ is given as $\gamma = 1 \dots n$.

The UKF procedure's subsequent step is to assess the transformed set of sigma points for each of the points using,

$$\boldsymbol{x}_l(k+1|k) = f\left[\boldsymbol{x}_l(k|k), k\right], \quad l = 0 \dots 2n. \tag{A.2}$$

The anticipated mean and covariance are then calculated using these transformed values.[26]

$$\hat{\boldsymbol{x}}(k+1|k) = \frac{1}{n+\kappa}\left\{\kappa \boldsymbol{x}_0(k+1|k) + \frac{1}{2}\sum_{l=1}^{2n} \boldsymbol{x}_l(k+1|k)\right\}, \tag{A.3a}$$

$$\begin{aligned} P(k+1|k) &= P^*(k+1|k) + Q(k) \\ &= \frac{1}{n+\kappa}\left\{\kappa\left[\boldsymbol{x}_0(k+1|k) - \hat{\boldsymbol{x}}(k+1|k)\right]\left[\boldsymbol{x}_0(k+1|k) - \hat{\boldsymbol{x}}(k+1|k)\right]^T\right. \\ &\quad \left. + \frac{1}{2}\sum_{l=1}^{2n}\left[\boldsymbol{x}_l(k+1|k) - \hat{\boldsymbol{x}}(k+1|k)\right]\left[\boldsymbol{x}_l(k+1|k) - \hat{\boldsymbol{x}}(k+1|k)\right]^T\right\} + Q(k). \end{aligned} \tag{A.3b}$$

Here, $\hat{\boldsymbol{x}}(k+1|k)$ is the predicted mean, $P(k+1|k)$ is the predicted covariance, $P^*(k+1|k)$ is the predicted covariance without the additive process noise.

Furthermore, the predicted observation vector is,

$$\hat{y}(k+1/k) = H(k+1)\hat{x}(k+1/k). \tag{A.4}$$

The observation covariance matrix is then calculated as follows,

$$P_{yy}(k+1/k) = H(k+1)P(k+1/k)H^T(k+1). \tag{A.5}$$

The cross-correlation matrix, on the other hand, can be found as,

$$P_{xy}(k+1/k) = P(k+1/k)H^T(k+1). \tag{A.6}$$

The UKF algorithm's update step comes next. The residual term $v(k+1)$ (or innovation sequence) is established at that stage as the difference between the actual observation and the predicted observation, initially by employing measurements $y(k+1)$,

$$v(k+1) = y(k+1) - \hat{y}(k+1|k), \tag{A.7}$$

The innovation covariance is,

$$P_{vv}(k+1|k) = P_{yy}(k+1|k) + R(k+1) = H(k+1)P(k+1/k)H^T(k+1) + R(k+1). \tag{A.8}$$

Here, $R(k+1)$ is the measurement noise covariance matrix. Equation is used to calculate the Kalman gain,

$$K(k+1) = P_{xy}(k+1|k)P_{vv}^{-1}(k+1|k). \tag{A.9}$$

Finally, the covariance matrix and updated states are determined by,

$$\hat{x}(k+1|k+1) = \hat{x}(k+1|k) + K(k+1)v(k+1), \tag{A.10}$$

$$P(k+1|k+1) = P(k+1|k) - P_{xy}(k+1/k)P_{vv}^{-1}(k+1|k)P_{xy}^T(k+1/k) \tag{A.11a}$$

or

$$P(k+1|k+1) = P(k+1|k) - K(k+1)P_{vv}(k+1|k)K^T(k+1). \tag{A.11b}$$

Here, $\hat{x}(k+1|k+1)$ is the estimated state vector and $P(k+1|k+1)$ is the estimated covariance matrix.